Check for updates

JGR Space Physics

RESEARCH ARTICLE
10.1029/2019JA027409

Martian Ionopause Boundary: Coincidence With Photoelectron Boundary and Response to Internal and External Drivers

F. Duru[1], N. Baker[1], M. De Boer[1], A. Chamberlain[1], R. Verchimak[1], D. D. Morgan[2], F. Chu[2], Z. Girazian[2], D. A. Gurnett[2], J. Halekas[2], and A. Kopf[2]

[1]Department of Physics, Coe College, Cedar Rapids, IA, USA, [2]Department of Physics and Astronomy, University of Iowa, Iowa City, IA, USA

Key Points:
- An ionopause boundary, defined as an altitudinal steep density gradient, has been detected in 13% of the cases in 12 years of MARSIS data
- In 89% of the cases, the ionopause coincides with the PEB
- The ionopause altitude is affected by solar wind dynamic pressure and crustal magnetic fields

Correspondence to:
F. Duru,
firdevs-duru@uiowa.edu

Citation:
Duru, F., Baker, N., De Boer, M., Chamberlain, A., Verchimak, R., Morgan, D. D., et al. (2020). Martian Ionopause boundary: Coincidence with photoelectron boundary and response to internal and external drivers. *Journal of Geophysical Research: Space Physics*, *125*, e2019JA027409. https://doi.org/10.1029/2019JA027409

Received 13 SEP 2019
Accepted 29 FEB 2020
Accepted article online 8 MAR 2020

©2020. American Geophysical Union. All Rights Reserved.

Abstract The Martian ionopause boundary detected as steep gradients in the local electron density profiles from the Mars Advanced Radar for Subsurface and Ionospheric Sounder on Mars Express is studied individually and statistically and compared to the photoelectron boundary identified by the drop of photoelectron signature due to CO_2 and O molecules. In ~90% of the cases where we have electron energy flux data, the ionopause coincides with the photoelectron boundary. The steep density gradients form at the border of the photoelectron region and above. The ionopause is observed in a wide range of latitude, longitude, and altitude. According to remote sounding investigations, the average thickness of the ionopause is ~30 km. The average altitude is between 500 and 700 km on the dayside. The altitude of the ionopause is inversely related to the solar wind dynamic pressure. Strong crustal magnetic fields increase the altitude of the boundary and they have a slight, negative effect on the occurrence only for high values. The ionopause occurs more frequently, and its altitude is higher during southern summer. The average altitude of the ionopause and solar irradiance are correlated with each other. The effect of the extreme ultraviolet flux on the occurrence rate is less noticeable.

1. Introduction

Understanding the interaction of the ionosphere of Mars with the solar wind provides information on the evolution and current mechanisms and the plasma environment of the planet. To achieve this, knowledge of the boundaries between Mars and solar wind and the physics behind them should be obtained. Lacking a global magnetic field (Acuna et al., 1998), Mars is more susceptible to the effects of the solar wind than planets with strong global magnetism such as Earth. Due to its high conductivity, the ionosphere acts as a barrier to the solar wind flow, causing many boundaries to form. A well-defined bow shock which is a collisionless shock standing between the solar wind and magnetosheath; a magnetic pile-up boundary (MPB), that separates the magnetic pile-up region from the magnetosheath—a sharp transition where the solar wind proton density drops sharply; and induced magnetospheric boundary (IMB), obtained by ion and electron measurements, that separates induced magnetosphere from the magnetosheath, are some examples of boundaries at Mars (Vignes et al., 2000; Trotignon et al., 2006; Nagy et al., 2004; Schunk & Nagy, 2009; Lundin et al., 2004; Duru et al., 2010).

Over the years, several boundaries in the environment of Mars have been identified and named according to the instruments and procedures used to define them. Some of these boundaries coincide with each other, at least under some conditions (Espley, 2018; Matsunaga et al., 2017).

Herein, we provide our results from the investigation of the ionopause boundary at Mars using 12 years of local electron density data from Mars Advanced Radar for Subsurface and Ionospheric Sounder (MARSIS) onboard Mars Express (MEX). Our purpose is to provide a more holistic view of the ionopause and understand the conditions that could change the occurrence rate and appearance of this boundary.

We define the ionopause boundary as a steep altitudinal gradient in the ionospheric density, in analogy with previous work from Venus. The Pioneer Venus orbiter data revealed sharp density drops in almost all the orbits (Brace et al., 1980; Elphic et al., 1980; Elphic et al., 1981). Duru et al. (2009) studied similar steep density gradients on the Martian ionosphere using MARSIS local electron density profiles and concluded that

21699402, 2020, 5, Downloaded from https://agupubs.onlinelibrary.wiley.com/doi/10.1029/2019JA027409 by University Of Iowa, Wiley Online Library on [17/11/2022]. See the Terms and Conditions (https://onlinelibrary.wiley.com/terms-and-conditions) on Wiley Online Library for rules of use; OA articles are governed by the applicable Creative Commons License

21699402, 2020, 5, Downloaded from https://agupubs.onlinelibrary.wiley.com/doi/10.1029/2019JA027409 by University Of Iowa, Wiley Online Library on [17/11/2022]. See the Terms and Conditions (https://onlinelibrary.wiley.com/terms-and-conditions) on Wiley Online Library for rules of use; OA articles are governed by the applicable Creative Commons License

the ionopause is a transient feature on Mars, happening only about 18% of the time. Vogt et al. (2015) analyzed the ionopause with the Neutral Gas and Ion Mass Spectrometer (NGIMS), Solar Wind Ion Analyzer (SWIA), and Solar Wind Electron Analyzer (SWEA) instruments onboard Mars Atmosphere and Volatile Evolution (MAVEN). Due to their more generous definition of steepness, they observed the ionopause in about 50% of the cases. Recently, Chu et al. (2019) studied the steep density gradients using MARSIS remote sounding data and showed that the occurrence rate is affected by the extreme ultraviolet (EUV) radiation and crustal magnetic fields.

Some studies have defined the ionopause differently. For example, Knudsen et al. (1979) defined the Venus ionopause as the location where the electron density first drops below about 100 cm^{-3}. Similarly, Han et al. (2014) used a 10^3 cm^{-3} density threshold to define the ionopause. We believe this kind of definition is open to ambiguity since the Martian ionosphere is highly fluctuating (Gurnett et al., 2010; Bougher et al., 2015). In many instances, the density drops and rises back to high values. We used the steep density gradient method with the density profiles to identify the ionopause and made sure that the density does not go back to ionospheric values after the ionopause.

2. Instruments

In this study, we define the ionopause using local electron density data from MARSIS, one of the six instruments on MEX (Chicarro et al., 2004), and study the cases we observe using ASPERA-3 ELS and MAVEN SWIA. MARSIS (Picardi et al., 2004) is a low-frequency radar, which performs remote sounding of the ionosphere and subsurface, by sending radio signals at 160 different frequencies between 100 kHz and 5 MHz and by recording the time it takes for the signal to be reflected back to the spacecraft. Remote sounding surveys the planet's ionosphere between altitudes of about 130 and 400 km. In addition, MARSIS can measure the electron density and the magnitude of the magnetic field at the spacecraft. To obtain the local electron density, the spacing between electron plasma oscillation harmonics are measured, which provides the local electron plasma frequency, which in turn can be converted into electron density using $f_p = 8980\sqrt{n_e}$, where f_p is in Hz and n_e is in cm^{-3} (Gurnett & Bhattacharjee, 2005). The harmonics are seen as equally spaced, vertical lines in the upper left corners of the plots of echo intensity as a function of time delay and frequency, which are called ionograms (Gurnett et al., 2005; Duru et al., 2008; Duru et al., 2019). The magnetic field magnitude is obtained by measuring the spacing between electron cyclotron echoes (Gurnett et al., 2005; Akalin et al., 2010).

The Analyzer of Space Plasma and Energetic Atoms (ASPERA-3) is another instrument onboard MEX. Its main objective is to study the near-Mars plasma environment (Barabash et al., 2004). A low-power electron spectrometer (ELS), which covers an electron energy range up to 20 keV/q is one of the units of ASPERA-3. The electron flux is measured over a 360° field of view (Frahm et al., 2006). Horizontal lines at energies between 20 and 30 eV in the electron flux spectra identify the photoelectron region. The lines are caused by the ionization of the atmospheric neutrals, CO_2 and O, by EUV photons from the Sun. The location at which the photoelectron peaks disappear is called the photoelectron boundary (PEB) (Mitchell et al., 2000; Mitchell et al., 2001; Lundin et al., 2004; Frahm et al., 2006).

Since 2015, we also have access to the data from the MAVEN mission, which is designed to study the upper ionosphere and solar wind environment of Mars. Its aims are to provide information about the escape processes, the evolution of the Martian atmosphere, its habitability, and climate (Jakosky et al., 2015). MAVEN consists of eight sensors, among which SWIA is designed to measure the velocity distribution of solar wind ions (Halekas et al., 2015).

3. Ionopause and Comparison With the Photoelectron Boundary

Local electron density profiles show fluctuations for a given pass; however, a general pattern is almost always present: The local electron density starts from a low or zero value at the highest altitude of the spacecraft. It increases as the spacecraft descends and reaches its maximum value around the periapsis, after which it decreases as the spacecraft ascends. In some passes, there is an altitude where the local electron density drops or rises suddenly, forming a steep gradient (see Figure 1a). We define this steep altitudinal density gradient as the ionopause.

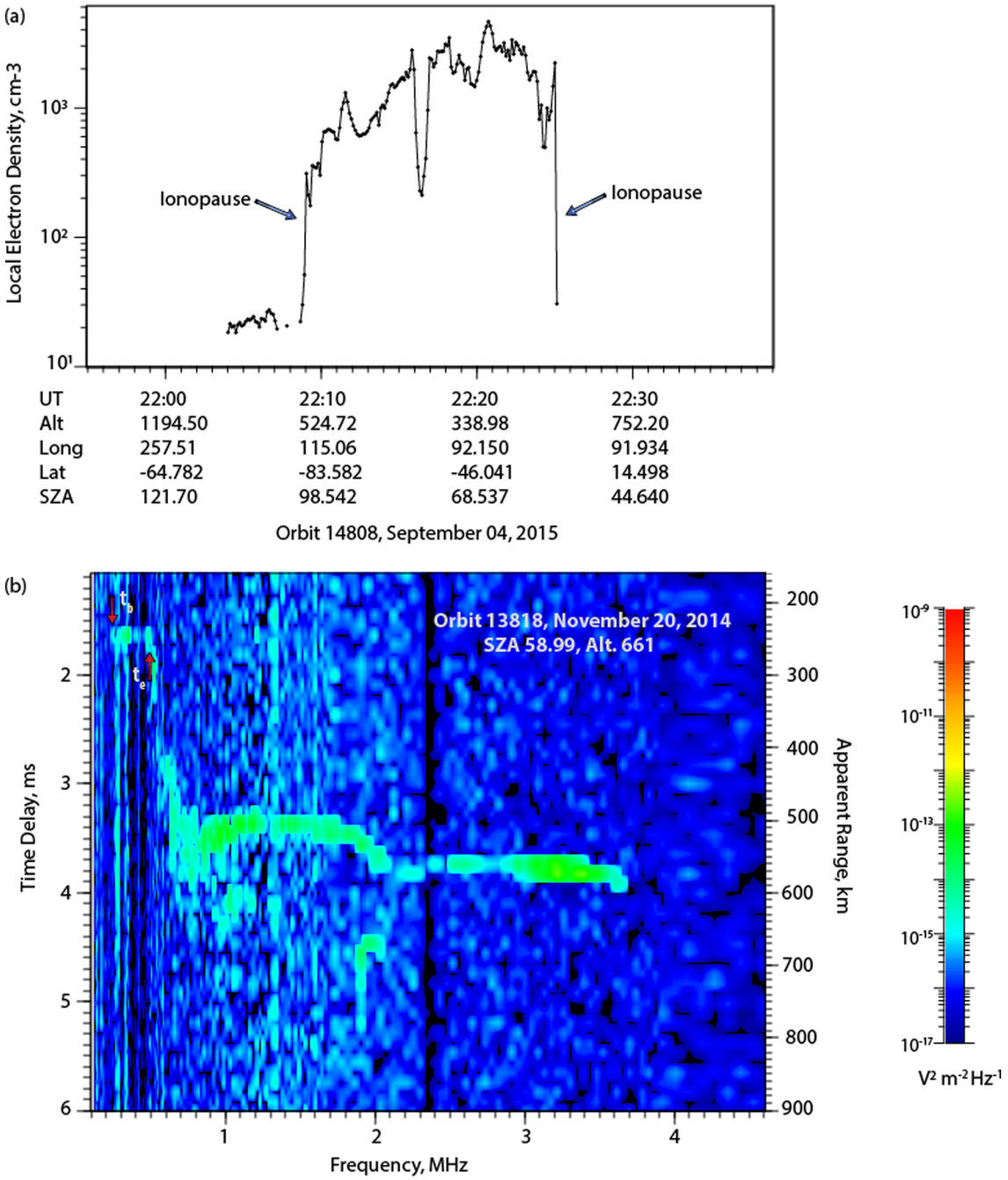

Figure 1. (a) The local electron density profile obtained with MARSIS for the pass on 4 September 2015. The two steep changes in the density are defined as ionopause. (b) An ionogram from an orbit from 20 November 2014. The short horizontal line at low frequencies and low time delays is the ionopause.

An example of the local electron density profile from 4 September 2015—orbit 14808—is shown in panel (a) of Figure 1. The pass starts at ~21:56 UT. The first electron plasma harmonics appear at ~22:04 UT. Therefore, it is not possible to obtain the local electron density value before this time. In the magnetosheath, the electron plasma oscillations do not consistently appear due to low density, high temperature, and/or high flow velocity (Duru et al., 2008). Once it is measurable, the local electron density stays almost constant at very low values of ~20 cm^{-3} until 22:09 UT, where it reaches 300 cm^{-3} in ~30 s. We identify the steep density gradient at ~22:09 UT and 22:25 UT as the ionopause. After the ionopause on the outbound leg, the local plasma oscillations disappear until the end of the pass.

21699402, 2020, 5, Downloaded from https://agupubs.onlinelibrary.wiley.com/doi/10.1029/2019JA027409 by University Of Iowa, Wiley Online Library on [17/11/2022]. See the Terms and Conditions (https://onlinelibrary.wiley.com/terms-and-conditions) on Wiley Online Library for rules of use; OA articles are governed by the applicable Creative Commons License

21699402, 2020, 5, Downloaded from https://agupubs.onlinelibrary.wiley.com/doi/10.1029/2019JA027409 by University Of Iowa, Wiley Online Library on [17/11/2022]. See the Terms and Conditions (https://onlinelibrary.wiley.com/terms-and-conditions) on Wiley Online Library for rules of use; OA articles are governed by the applicable Creative Commons License

We went through all the orbits and chose the ones that have steep density gradient with equal or more than 50 cm^{-3} within a single 7.54 s sweep period, which corresponds to a minimum slope of 5 cm^{-3}/km. Out of the ~3,700 orbits investigated—between August 2005 and November 2018—we identified 935 ionopause crossings with this method, which is ~7 times the number what in our previous study (Duru et al., 2009). However, given the longer time range, the occurrence rate derived from the current study is consistent with what is our previous results, with the ionopause identified in ~13% of the possible cases.

The ionopause can also be observed by remote sounding with MARSIS. The steep density gradients show up as a short horizontal line at low frequencies, below about 0.5 MHz, with the ionospheric echo being observed at higher frequencies and longer time delays (Duru et al., 2008; Chu et al., 2019). To detect the ionopause remotely, it has to be below the spacecraft. Since the ionograms are full of other features, such as local electron plasma harmonics, electron cyclotron echoes, oblique reflections, and so forth, it is not always possible to detect these short lines. When present, the short horizontal line usually lasts for a few consecutive ionograms, providing a clear and unambiguous indication of a steep density gradient.

We observed an ionopause crossing in 1,300 ionograms. An ionogram with the ionopause feature, from 20 November 2014, is shown in Figure 1b. The short horizontal line, at frequencies 0.3–0.55 MHz, shown between two red arrows, at a time delay of ~1.6 ms is the steep density gradient, observed before the ionospheric echo at about 3.4 ms.

The MARSIS local electron density profile from the pass from 8 August 2005 (orbit 1994) is shown in the top panel of Figure 2. The plot displays two well-defined steep density gradients in both the inbound and outbound segments of the orbit. The electron plasma harmonics are not observed until 01:57 UT. After this time, the local electron density increases as the spacecraft moves toward periapsis and then decreases back as it ascends. The change in the electron density is relatively smooth except at ~01:57 UT and ~02:15 UT, where we observe the two sharp density changes. After the sharp decrease at 2:15 UT, the electron plasma oscillations disappear for ~3 min. When the oscillations return, the density is low, below 100 cm^{-3}, and stays low until the end of the pass at 2:48 UT.

The magnitude of the local magnetic field for the orbit 1994 is shown in the bottom panel of Figure 2. On Venus, the location of the ionopause is typically characterized by a balance between the thermal ionospheric pressure below and magnetic pressure above. At the Venus ionopause, the magnetic field increases suddenly, coincident with a sudden drop in the electron density (Brace et al., 1980). In about half of the cases observed by Vogt et al. (2015), the magnetic field changes drastically in the vicinity of the ionopause. This behavior is not observed in MARSIS data. As seen in the figure, the magnetic field continues to change slowly as the spacecraft crosses the ionopause, which is a common feature of our cases.

The middle panel of Figure 2 displays the electron flux as a function of energy and time from ASPERA-3 ELS. At low altitudes in the ionosphere, the photoelectron signature due to the ionization of the atmospheric neutrals by the EUV and soft X-ray photons from the Sun is observed, at energies between 21 and 24 eV and 27 eV, due to the ionization of neutrals. Due to the instrumental energy resolution, the two lines are often observed as one (Frahmn et al., 2006; Mantas & Hanson, 1979). The photoelectron boundary (PEB), as identified by the disappearance of these horizontal lines, separates the ionospheric electrons from shocked magnetosheath electrons (Lundin et al., 2004). Above the PEB, higher energy electrons are observed, in some cases immediately after PEB, in others after a gap. As seen by the dashed lines in the figure, both ionopause cases identified with local electron density data from MARSIS correspond to the location of the PEB as seen by ELS, where the horizontal photoionization lines are lost and the high energy electrons are detected right after the ionopause.

Figure 3 shows a collection of ionopause crossings from different times during the mission, with corresponding ELS data also shown in this figure. The dashed lines show the location of the ionopause and where it corresponds in the electron energy data. In panels (a), (c), and (d), the ionopause is seen in both the inbound and outbound segments. On the other hand, in panels (b), (e), and (f), the steep density gradients are observed in only one of the orbit segments. One thing common to all six passes is that the ionopause location coincides with the PEB.

Regardless of their presence in one or both legs, 87% of all the ionopause cases for which the electron data were available occurred at the same location as the PEB for the cases we had ASPERA-3 data with clear

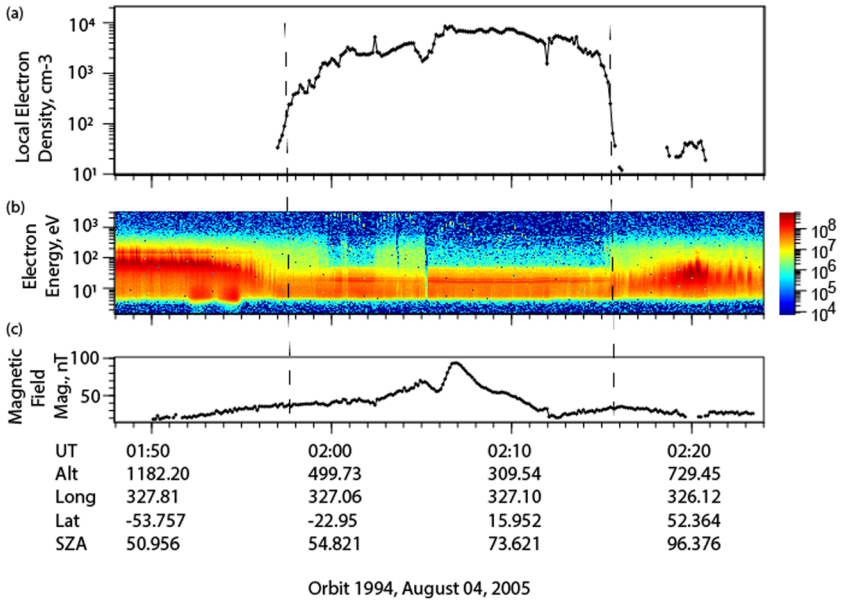

Figure 2. A pass for orbit 1994 from 4 August 2005. (a) The local electron density profile from MARSIS. (b) Electron energy flux from ASPERA-3 ELS. (c) The magnitude of the magnetic field from MARSIS. The dashed lines indicate the location of the ionopause cases.

PEB signatures. As seen in the examples, the coincidence is almost perfect between the position of the PEB and the steep density gradient. In every case, the ionopause altitude was lower than the altitude of the magnetosheath. In some cases, the magnetosheath started right after the PEB; in others, there was a gap between the two. A similar 4–5 min gap was also reported in Duru et al. (2009). In 6% of the cases, the photoelectron signature continued after the ionopause. According to Dubinin et al. (2006), the existence of this gap in the majority of cases is a clear indication of the fact that PEB and MPB are two distinct boundaries.

This does not mean that a steep density gradient would be observed every time the PEB is seen. When the PEB altitude is high, the electron densities are already low in the region. Without a high density at the beginning, it is not possible to obtain a sharp and sudden drop as the ones accepted as ionopause in this study. The pass from 7 August 2005 on panel (e) of Figure 3 is an example of this. On the inbound leg, the PEB is observed at an altitude of 480 km and SZA of 52°, and a sharp density gradient is present at the same time. However, on the outbound leg, the photoelectron signature continues even after 1,300 km of altitude. At that point, the local electron density is already too low to present a sudden drop.

4. Location of the Ionopause

Figure 4 shows the geographical locations of all the ionopause crossings identified from local electron density measurements. The background color indicates the magnitude of the crustal magnetic field at 400 km, from Morschhauser et al. (2014). The occurrence rate is slightly less near the poles; however, the difference is not very significant. Considering the data coverage is homogeneous with respect to geographic longitude (Chu et al., 2019), we find no evidence for an inhomogenous distribution of ionopause locations. We find that the ionopause occurs with approximately the same frequency at all latitudes and longitudes.

The average altitude of the ionopause, with the error bars, for a given solar zenith angle (SZA) range is shown in Figure 5a, along with the individual cases around Mars (Figure 5b). The average altitude is ~620 km around the subsolar point and goes down to ~510 km at 25°. Except at 65°, where it is about 570 km, the ionopause altitude is above 600 km until the deep nightside, where the data are much more scarce. The average altitudes are in agreement with the altitude of the PEB in Han et al. (2014).

21699402, 2020, 5, Downloaded from https://agupubs.onlinelibrary.wiley.com/doi/10.1029/2019JA027409 by University Of Iowa, Wiley Online Library on [17/11/2022]. See the Terms and Conditions (https://onlinelibrary.wiley.com/terms-and-conditions) on Wiley Online Library for rules of use; OA articles are governed by the applicable Creative Commons License

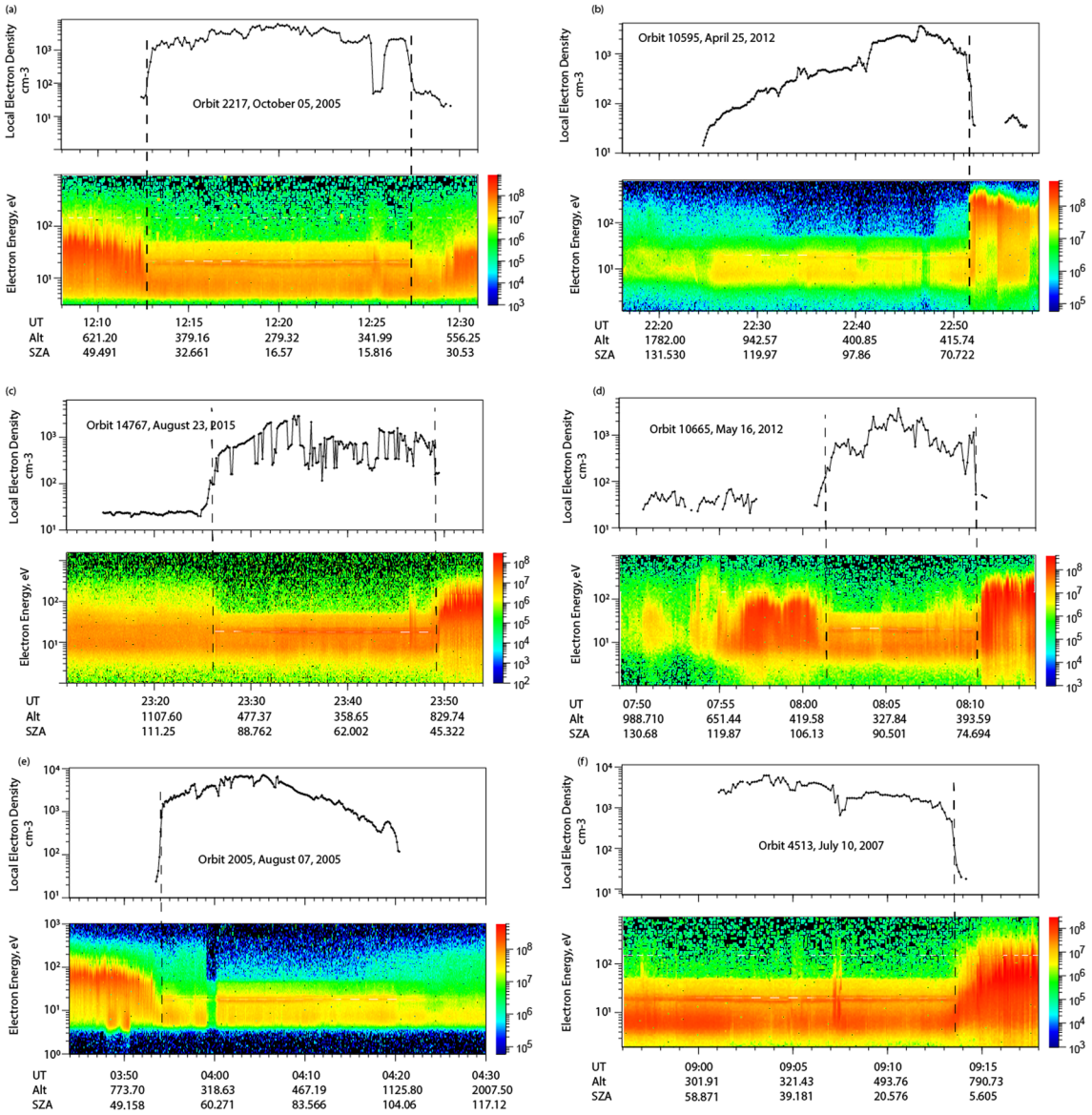

Figure 3. A collection of MARSIS local electron density profiles along with ASPERA-3 ELS electron energy spectra for six passes.

5. Effect of the Solar Wind Dynamic Pressure

It is expected that as the solar wind dynamic pressure increases, the altitude of the boundaries decreases. Recently, Garnier et al. (2017) showed that there is a clear relationship between the solar wind ram pressure and the average altitude of the PEB. According to their findings, which used MAVEN data, the altitude of PEB is ~700 km for very low ram pressure and decreases to ~500 km at 2.5 nPa.

We plotted the average altitude of the steep density gradients, from local electron densities, as a function of the solar wind dynamic pressure obtained by the MAVEN SWIA instrument, available since November 2014 (Figure 6). The pressure values used are the closest values in time to the ionopause for up to 6 hr. The cases where the two values are more than 6 hr apart are excluded. As Figure 6 shows, the average altitude of the ionopause is at ~680 km at 0.25 nPa ram pressure and decreases to ~480 km at 1.75 nPa ram pressure. The shape of the plot is strikingly similar to that of Garnier et al. (2017) for all pressure values. The values are somewhat lower in our results, but the difference is usually within 50 km. These findings suggest that the ionopause coincides with PEB. The ionopause and PEB have similar altitudes, and they behave in the same way with changing solar wind dynamic pressure.

21699402, 2020, 5, Downloaded from https://agupubs.onlinelibrary.wiley.com/doi/10.1029/2019JA027409 by University Of Iowa, Wiley Online Library on [17/11/2022]. See the Terms and Conditions (https://onlinelibrary.wiley.com/terms-and-conditions) on Wiley Online Library for rules of use; OA articles are governed by the applicable Creative Commons License

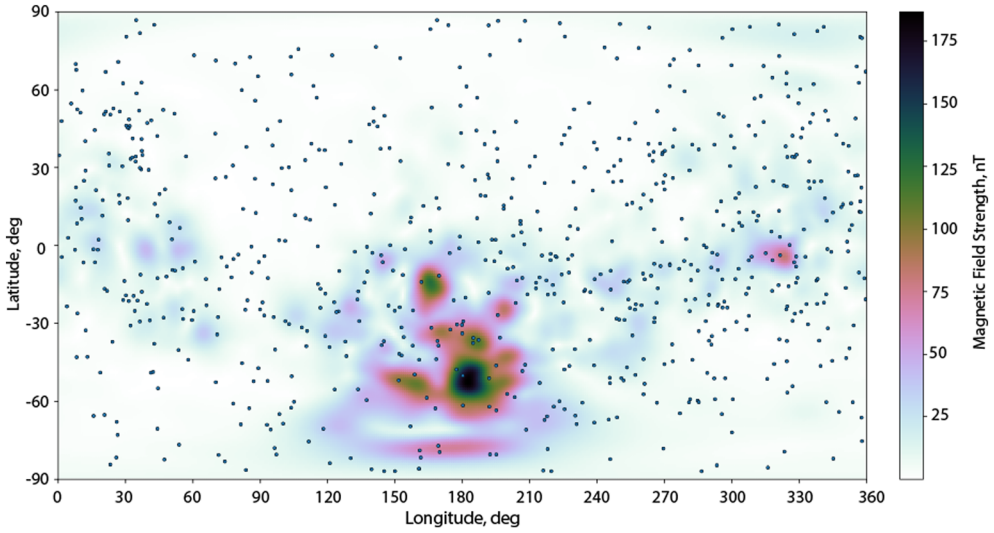

Figure 4. Geographic distribution of the ionopause cases. Individual ionopause crossings are shown on the magnetic field magnitude map of Mars.

6. Effect of the Crustal Fields on the Occurrence and the Altitude of the Ionopause

The crustal fields are known to increase the local altitude of the boundaries at Mars (Crider et al., 2002; Brain et al., 2005), as well as the average values of electron densities at a given altitude (Andrews et al., 2014; Flynn et al., 2017). Figure 7 confirms the previous results for the dayside: The altitude of the ionopause at a given SZA range is higher above regions of strong crustal fields on the dayside. In this figure, the green and orange dots represent the average altitude of the cases above weak crustal field regions (less than 50 nT) and above strong crustal field locations (more than 50 nT), respectively. The ionopause altitude above the strong crustal fields is higher on the dayside, by more than 200 km for some SZA ranges. This result is also consistent with Garnier et al. (2017), who showed that the altitude of the PEB depends strongly on the crustal magnetic fields, which increase the altitude on average by about 150 km, and with Chu et al. (2019) who found that the crustal magnetic fields increase the altitude of the ionopause by ~1.58 km per nT.

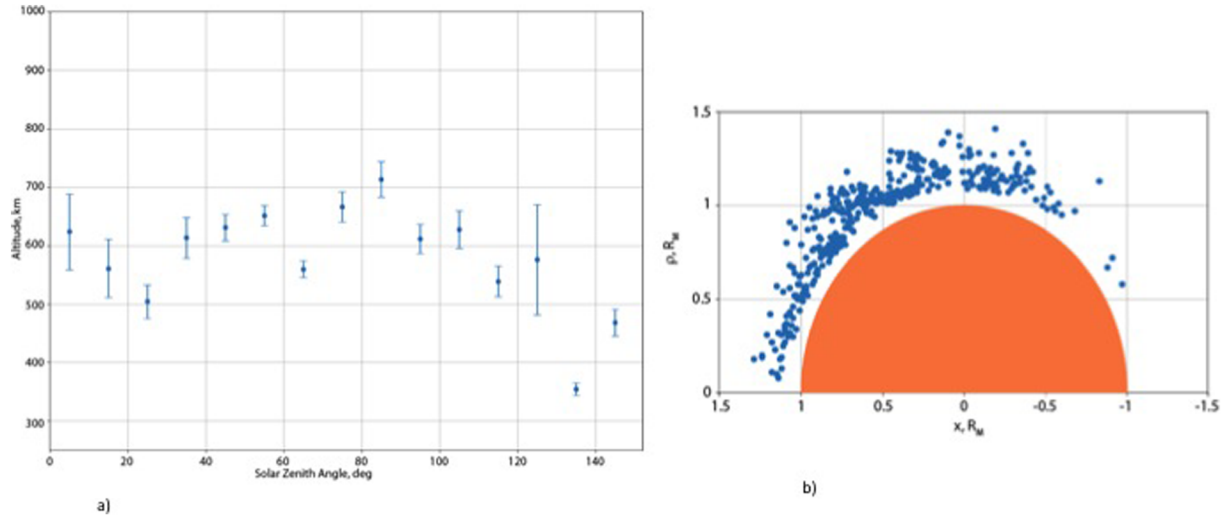

Figure 5. (a) Average altitude and the error bars of the ionopause as a function of the solar zenith angle with 10 deg of SZA bins. (b) The location of individual ionopause cases around Mars.

21699402, 2020, 5, Downloaded from https://agupubs.onlinelibrary.wiley.com/doi/10.1029/2019JA027409 by University Of Iowa, Wiley Online Library on [17/11/2022]. See the Terms and Conditions (https://onlinelibrary.wiley.com/terms-and-conditions) on Wiley Online Library for rules of use; OA articles are governed by the applicable Creative Commons License

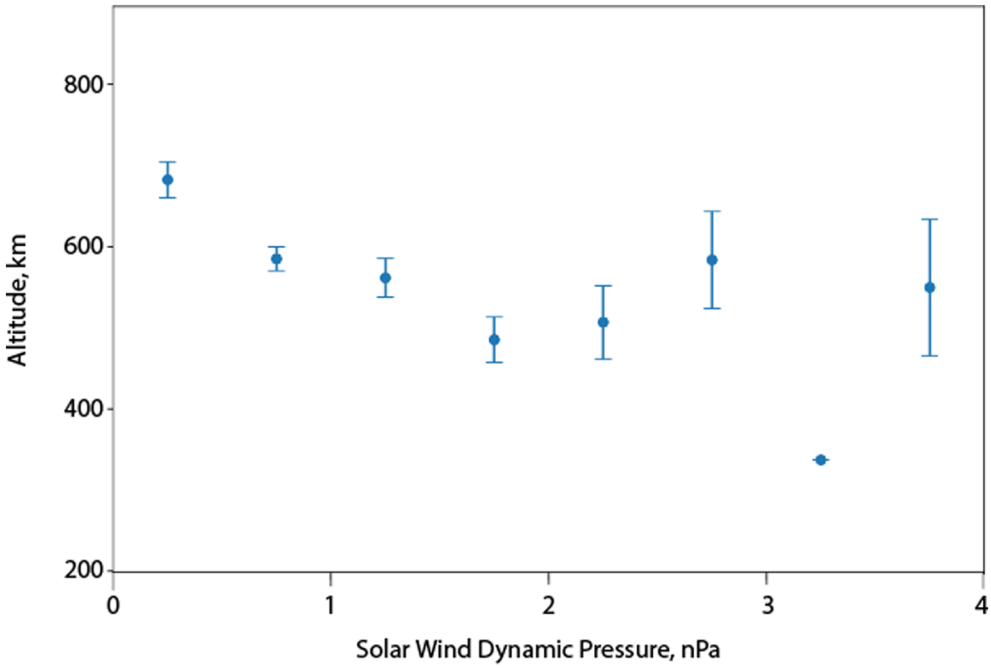

Figure 6. The average altitude with error bars of the ionopause as a function of solar wind dynamic pressure computed with MAVEN SWIA.

Another interesting question is whether crustal fields have an effect on the occurrence of the ionopause. To answer this question, we made histograms of the ratio between the occurrence of the ionopause crossings over areas with crustal magnetic fields higher than a given magnetic field value (10, 50, and 125 nT) and the percentage of the total area on Mars with crustal magnetic fields higher than the given value. Again, the magnetic field magnitude at 400 km is used (Morschhauser et al., 2014). According to Figure 8, the ratio between the ionopause occurrence and the percentage of Mars' area with magnetic field >10 nT is about 1.37. The ratio becomes 1.08 for >50 nT, and it is 0.82 for >120 nT. Since our data coverage is fairly homogeneous, these plots tell us that there is no substantial effect of the crustal fields on the occurrence. However,

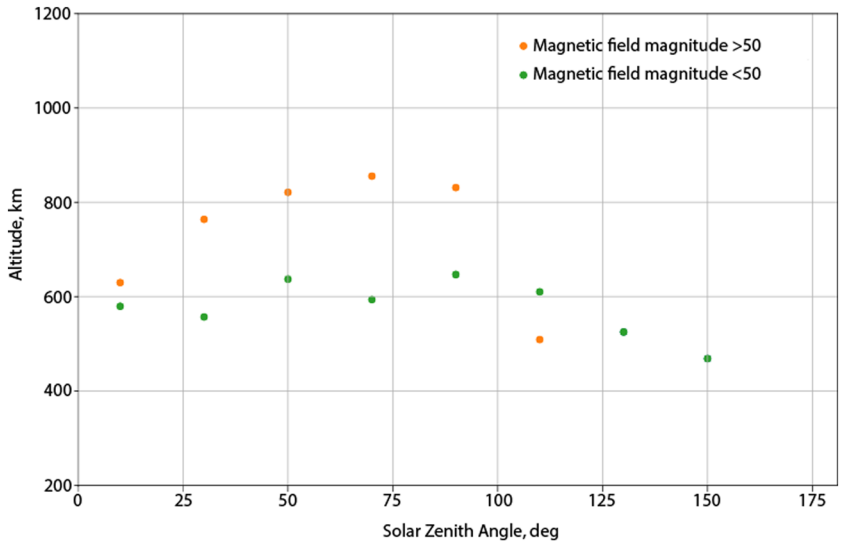

Figure 7. The average altitude of the ionopause above strong crustal magnetic field region (orange points) and weak crustal magnetic field regions (green dots). The border of the crustal magnetic fields is 50 nT at 400 km.

21699402, 2020, 5, Downloaded from https://agupubs.onlinelibrary.wiley.com/doi/10.1029/2019JA027409 by University Of Iowa, Wiley Online Library on [17/11/2022]. See the Terms and Conditions (https://onlinelibrary.wiley.com/terms-and-conditions) on Wiley Online Library for rules of use; OA articles are governed by the applicable Creative Commons License

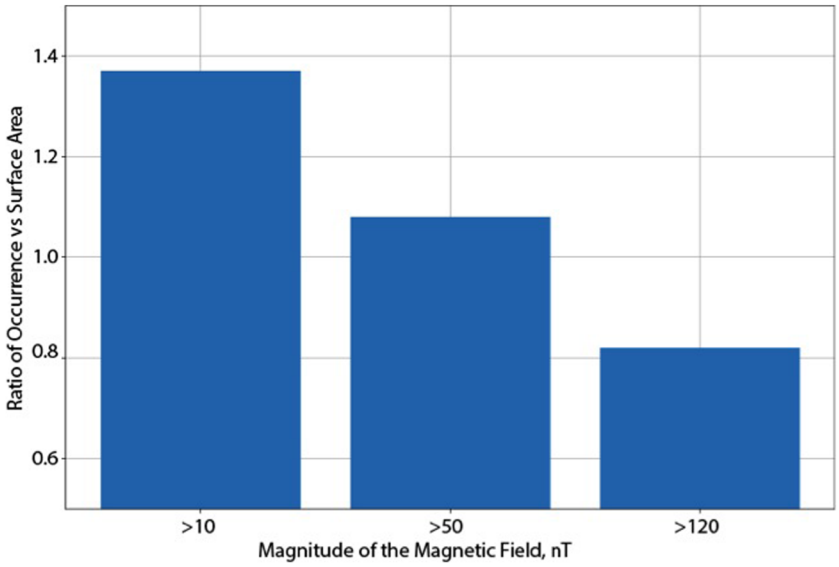

Figure 8. The ratio of the percentage of the occurrence of ionopause over a region of magnetic field higher than a given value to the percentage of area of Mars with magnetic fields stronger than the given value. The magnetic field strengths chosen are 10, 50, and 120 nT.

as the crustal field magnitude becomes high, it may prevent the formation of the steep density gradients. According to Chu et al. (2019), the crustal fields have a clear negative effect on the formation of the ionopause. Although we do not find a strong correlation in our data, we can say that there may be a slight effect for crustal field values greater than 100 nT at 400 km.

7. Effect of Seasons and Solar Cycle

The EUV photon fluxes have been shown to have an effect on the altitude of the boundaries at Mars. Garnier et al. (2017) showed that the PEB is raised when the EUV flux is high. However, Mitchell et al. (2001), who made the observation of the PEB during solar minimum with Electron Reflectometer on Mars Global Surveyor data, did not observe any effect of the EUV flux on the ionopause altitude.

Mars experiences all four seasons. Due to Mars' orbit, the seasonal variations include significant variations in the Mars-Sun distance and, thus, EUV flux level. Seasons affect the temperature, electron, ion, and peak densities in the ionosphere, as well as the occurrence rates of pickup ions, hydrogen corona, H escape rates, and so forth (Valeille et al., 2009; Yamauchi et al., 2015; Halekas et al., 2017; Rahmati et al., 2018; Girazian et al., 2019).

Investigation of the average altitude of the ionopause boundary for Northern Hemisphere seasons revealed that the altitude does not change substantially with the seasons. We find that there is ~17 km of altitude difference between winter (628 km on average) and summer (611 km on average). Northern Hemisphere winter corresponds to Southern Summer, including the perihelion, where the effect of the Sun is more prominent.

The occurrence rate of the ionopause cases (calculated by dividing the number of ionopause crossings to the total data) also changes slightly with seasons. Again, the effect is mostly due to the EUV flux changes and dust storms during Southern summer. The occurrence is slightly higher during northern winter (about 0.145), where EUV flux should be higher, which in turn can cause more clear photoelectron signatures. The occurrence rate is slightly below 0.1 for the northern summer.

Recent studies show that the solar cycle has significant effects on the composition, scale height, and density distribution of the ionosphere (Morgan et al., 2008; Bougher et al., 2015; Sanchez-Cano et al., 2016; Lundin et al., 2013; Withers et al., 2014). Figure 9 displays the average altitude of the ionopause as a function of time (top panel), the occurrence rate of the ionopause cases as a function of the universal time (middle panel), and

21699402, 2020, 5, Downloaded from https://agupubs.onlinelibrary.wiley.com/doi/10.1029/2019JA027409 by University Of Iowa, Wiley Online Library on [17/11/2022]. See the Terms and Conditions (https://onlinelibrary.wiley.com/terms-and-conditions) on Wiley Online Library for rules of use; OA articles are governed by the applicable Creative Commons License

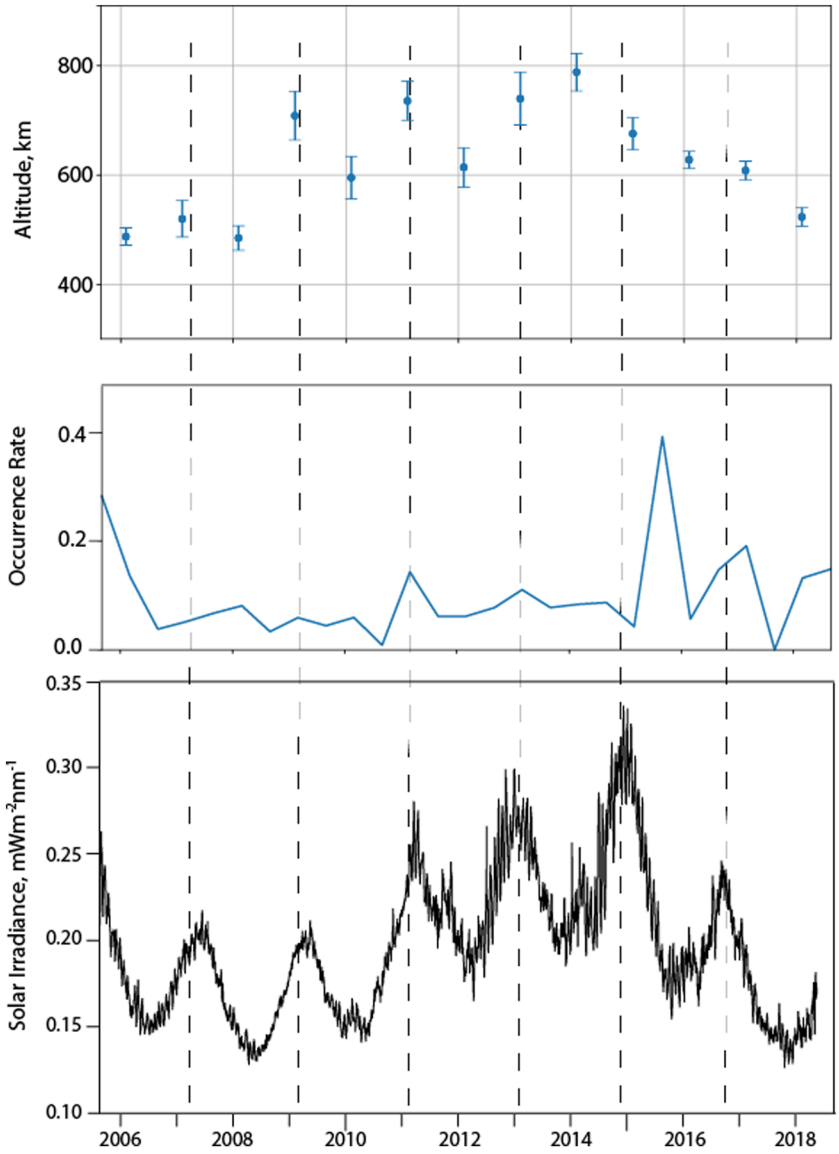

Figure 9. Top panel: The average altitude of the ionopause as a function of time. Middle panel: The occurrence rate of the ionopause as a function of time. Bottom panel: Solar irradiance corrected for Mars as a function of time from TIMED-SEE data.

the solar irradiance at 30.5 nm from Thermosphere, Ionosphere, Mesosphere Energetics, and Dynamics-Solar EUV Experiment (TIMED-SEE) scaled to Mars' distance (bottom panel). Since both the average altitude and the occurrence rate are calculated for all the data, they include variations due to parameters other than the EUV, as well. However, even then, it is possible to see a correlation between the altitude of the ionopause and the solar irradiation. The relation of the occurrence rate to the solar irradiation is weak, but the effect is observed for most of the solar cycle. These results are in agreement with previous results showing that the EUV increases the height of the ionosphere and the boundaries (Duru et al., 2019; Garnier et al., 2017; Girazian et al., 2019; Chu et al., 2019).

8. Conclusions

The ionopause boundary, defined as a steep altitudinal density gradient, is a transient feature at Mars. According to this study, which is performed using MARSIS local electron density profiles, the ionopause crossings occurs less than 15% of the time. The percentage is higher in some previous studies, such as

21699402, 2020, 5, Downloaded from https://agupubs.onlinelibrary.wiley.com/doi/10.1029/2019JA027409 by University Of Iowa, Wiley Online Library on [17/11/2022]. See the Terms and Conditions (https://onlinelibrary.wiley.com/terms-and-conditions) on Wiley Online Library for rules of use; OA articles are governed by the applicable Creative Commons License

Vogt et al. (2015) who observed the ionopause in about 50% of the cases, due to their less strict criteria in defining the steepness.

MARSIS observations confirm that, unlike at Venus, at Mars the ionopause does not usually represent a balance between the thermal ionospheric pressure and magnetic field pressure. The ionospheric thermal pressure in the Martian ionosphere is often insufficient to balance the total pressure above it during solar minimum (Nagy et al., 2004; Sanchez-Cano et al., 2016). However, it can be strong enough to withstand the incident solar wind dynamic pressure during solar maximum (Nagy et al., 2004; Zhang & Luhmann, 1992). This may be one of the reasons why the physics of the ionopause at Mars is different than that of Venus.

Comparisons with electron energy flux data from ASPERA-3 ELS show that in 90% of cases the ionopause occurs where the photoelectron signature in the ionosphere appears/disappears, that is, at the PEB. This fact is consistent with Mitchell et al. (2001) who stated that the PEB and ionopause boundaries are closely related to each other. However, it disagrees with the findings of Han et al. (2014), who found that the ionopause boundary is about 200 km lower than the PEB on average. The discrepancy is likely due to our definitions of ionopause. Han et al. (2014) defined the location of the ionopause the altitude where the electron density reaches 10^3 cm^{-3}, without a steep gradient requirement, and regardless of whether the density returns to high values afterward. Recently, Han et al. (2019) reported that the steep density gradients and PEB coincide whenever they are observed together. However, they found that the average altitude of the PEB is higher than the average altitude of the steep density gradients.

We find that the ionopause altitude on the dayside varies between ~500 and 700 km on the dayside, similar to the average altitude of the PEB (Han et al., 2014). Also, consistent with previous studies on the effect of solar wind dynamic pressure on the altitude of the boundaries at Mars, the altitude of the ionopause boundary decreases with increasing solar wind pressure. Strong crustal magnetic fields also increase the altitude of the ionopause by a substantial amount, up to 200 km in some SZA ranges. Moreover, the comparison of the percentage of the Mars area with the magnetic fields above a given value and the percentage of the ionopause cases at locations with a magnetic field above a given value shows that the strong magnetic fields (above 50 nT, at 400 km) could have a negative effect on the occurrence of the ionopause boundary. Chu et al. (2019) explained this in terms of the pressure due to crustal fields, which does not require a big increase in the thermal pressure to counteract the solar wind pressure.

During northern winter, which occurs just after perihelion at Mars, we find higher ionopause altitudes, as well as higher occurrence rates. A fairly clear correlation is observed between the average altitude of the ionopause and the solar irradiance. The relation is less noticeable for the occurrence rate.

Our results confirm previous studies that show that the altitudes of the boundaries are affected by several parameters, such as EUV, crustal fields, and solar wind dynamic pressure.

Acknowledgments
TIMED-SEE data are from the University of Colorado (http://lasp.colorado.edu/lisird/index.html). Work at Iowa was supported by NASA through Contract 1224107 from the Jet Propulsion Laboratory. MARSIS and ASPERA-3 data are available through the Planetary Data System (http://pds-geosciences.wustl.edu). All MAVEN data are available through the Planetary Data System (http://ppi.pds.nasa.gov).

References

Acuna, M., Connerney, J. E. P., Wasilewski, P., Lin, R. P., Anderson, K. A., Carlson, C. W., et al. (1998). Magnetic field and plasma observations at Mars: Initial results of the Mars global surveyor mission. *Science*, *279*(5357), 1676–1680.

Akalin, F., Morgan, D. D., Gurnett, D. A., Kirchner, D. L., Brain, D. A., Modolo, R., et al. (2010). Dayside induced magnetic field of the ionosphere of Mars. *Icarus*, *206*, 104–111.

Andrews, D. J., Edberg, N. J. T., Eriksson, A. I., Gurnett, D. A., Morgan, D., Nemec, F., & Opgenoorth, H. J. (2014). Control of the topside Martian ionosphere by the crustal magnetic fields. *Journal of Geophysical Research: Space Physics*, *120*, 3042–3058. https://doi.org/10.1002/2014JA020703

Barabash, S., Lundin, R., Andersson, H., Gimholt, J., Holmström, M., Norberg, O., et al. (2004), ASPERA-3: Analyzer of space plasmas and energetic ions for Mars Express, Mars Express: The scientific payload. Ed. by Andrew Wilson, Scientific coordination: Agustin Chicarro. *ESA SP-1240*, Noordwijk, Netherlands: ESA Publications Division, ISBN 92–9092–556-6, 2004, p. 121–139.

Bougher, S. W., Jakosky, B., Halekas, J., Grebowsky, J., Luhmann, J., Mahaffy, P., et al. (2015). Early MAVEN Deep Dip campaign reveals thermosphere and ionosphere variability. *Science*, *350*, 6261. https://doi.org/10.1126/science.aas0459

Bougher, S. W., Pawlowski, D., Bell, J. M., Nelli, S., McDunn, T., Murphy, J. R., et al. (2015). Mars Global Ionosphere-Thermosphere Model: Solar cycle, seasonal, and diurnal variations of the Mars upper atmosphere. *Journal of Geophysical Research: Planets*, *120*, 311–342. https://doi.org/10.1002/2014JE004715

Brace, L. H., Theis, R. F., Hoegy, W. R., Wolfe, J. H., Mihalov, J. D., Russell, C. T., et al. (1980). The dynamic behavior of the Venus ionosphere in response to solar wind interactions. *Journal of Geophysical Research*, *85*, A13, 7663–7678.

Brain, D. A., Halekas, J. S., Lillis, R., Mitchell, D. L., Lin, R. P., & Crider, D. H. (2005). Variability of the altitude of the Martian sheath. *Geophysical Research Letters*, *321*, L18203. https://doi.org/10.1029/2005GL023126

Chicarro, A., Martin, P., & Traunter, R. (2004). Mars Express: A European mission to the red planet. In A. Wilson (Ed.), *Mars Express, The Scientific Payload*, Vol. 1240 (pp. 3–16). Noordwijk, Netherlands: ESA Publication Division.

21699402, 2020, 5, Downloaded from https://agupubs.onlinelibrary.wiley.com/doi/10.1029/2019JA027409 by University Of Iowa, Wiley Online Library on [17/11/2022]. See the Terms and Conditions (https://onlinelibrary.wiley.com/terms-and-conditions) on Wiley Online Library for rules of use; OA articles are governed by the applicable Creative Commons License

Chu, F., Girazian, Z., Gurnett, D. A., Morgan, D. D., Halekas, J., Kopf, A. J., et al. (2019). The effect of crustal magnetic fields and solar EUV flux on ionopause formation at Mars. *Geophysical Research Letters*, *46*, 10,257–10,266. https://doi.org/10.1029/2019GL083499

Crider, D. H., Acuña, M. H., Connerney, J. E. P., Vignes, D., Ness, N. F., Krymskii, A. M., et al. (2002). Observations of the latitude dependence of the location of the Martian magnetic pileup boundary. *Geophysical Research Letters*, *29*(8), 11-1–11-4. https://doi.org/10.1029/2001GL013860

Dubinin, E., Fränz, M., Woch, J., Roussos, E., Barabash, S., Lundin, R., et al. (2006). Plasma morphology at Mars. ASPERA-3 observations. *Space Science Review*, *126*(1-4), 209–238. https://doi.org/10.1007/s11214-006-9039-4

Duru, F., Brain, B., Gurnett, D. A., Halekas, J., Morgan, D. D., & Wilkinson, C. J. (2019). Electron density profiles in the upper ionosphere of Mars from 11 years of MARSIS data: Variability due to seasons, solar cycle and crustal magnetic fields. *Journal of Geophysical Research: Space Physics*, *124*, 3057–3066. https://doi.org/10.1029/2018JA026327

Duru, F., Gurnett, D. A., Frahm, R. A., Winningham, J. D., Morgan, D. D., & Howes, G. G. (2009). Steep, transient density gradients in the Martian ionosphere similar to the ionopause at Venus. *Journal of Geophysical Research*, *114*, A12310. https://doi.org/10.1029/2009JA014711

Duru, F., Gurnett, D. A., Morgan, D. D., Modolo, R., Nagy, A. F., & Najib, D. (2008). Electron densities in the upper ionosphere of Mars from the excitation of electron plasma oscillations. *Journal of Geophysical Research*, *113*, A07302. https://doi.org/10.1029/2008JA013073

Duru, F., Gurnett, D. A., Winningham, J. D., Frahm, R., & Modolo, R. (2010). A plasma flow velocity boundary at Mars from the disappearance of electron plasma oscillations. *ICARUS*, *206*, 74–82. https://doi.org/10.1016/j.icarus.2009.04.012

Elphic, R. C., Russell, C. T., Luhmann, J. G., Scarf, F. L., & Brace, L. H. (1981). The Venus ionopause current sheet: Thickness length scale and controlling factors. *Journal of Geophysical Research*, *86*, A13.

Elphic, R. C., Russell, C. T., Slavin, J. A., & Brace, L. H. (1980). Observations of the dayside ionopause and ionosphere of Venus. *Journal of Geophysical Research*, *85*, A13.

Espley, J. R. (2018). The Martian magnetosphere: Areas of unsettled terminology. *Journal of Geophysical Research: Space Physics*, *123*, 4521–4525. https://doi.org/10.1029/2018JA025278

Flynn, C. L., Vogt, M. F., Withers, P., Andersson, L., England, S., & Liu, G. (2017). MAVEN Observations of the effect of crustal magnetic fields on the electron density and temperature in the Martian dayside ionosphere. *Geophysical Research Letters*, *44*, 10,812–10,821. https://doi.org/10.1002/2017GL075367

Frahm, R. A., Sharber, J. R., Winningham, J. D., Wurz, P., Liemohn, M. W., Kallio, E., et al. (2006). Location of atmospheric photoelectron energy peaks within the Mars environment. *Space Science Reviews*, *126*, 389. https://doi.org/10.1007/s11214-006-9119-5

Garnier, R., Steckiewicz, M., Mazelle, C., Xu, S., Mitchell, D., Holmberg, M. K. G., et al. (2017). The Martian photoelectron boundary as seen by MAVEN. *Journal of Geophysical Research: Space Physics*, *122*, 10,472–10,485. https://doi.org/10.1002/2017JA024497

Girazian, Z., Mahaffy, P., Lee, Y., & Thiemann, E. M. B. (2019). Seasonal, solar zenith angle, and solar flux variations of O^+ in the topside ionosphere of Mars. *Journal of Geophysical Research: Space Physics*, *124*, 3125–3138. https://doi.org/10.1029/2018JA026086

Gurnett, D. A., & Bhattacharjee, A. (2005). *Introduction to plasma physics with space and laboratory applications*. Cambridge: Cambridge University Press.

Gurnett, D. A., Kirchner, D. L., Huff, R. L., Morgan, D. D., Persoon, A. M., Averkam, T. F., et al. (2005. Radar soundings of the ionosphere of Mars. *Science*, *310*, 1929–1933.

Gurnett, D. A., Morgan, D. D., Duru, F., Akalin, F., Winningham, J. D., Frahm, R. A., et al. (2010). Large density fluctuations in the Martian ionosphere as observed by the Mars Express radar sounder. *Icarus*, *206*, 83–94.

Halekas, J. S., Ruhunusiri, S., Harada, Y., Collinson, G., Mitchell, D. L., Mazelle, C., et al. (2017). Structure, dynamics, and seasonal variability of the Mars-solar wind interaction: MAVEN Solar Wind Ion Analyzer in-flight performance and science results. *Journal of Geophysical Research: Space Physics*, *122*, 547–578. https://doi.org/10.1002/2016JA023167

Halekas, J. S., E. R. Taylor, G. Dalton, G. Johnson, D. W. Curtis, J. P. McFadden, et al. (2015), The solar wind ion analyzer for MAVEN, *Space Science Reviews*, *195*, 125–151, doi:https://doi.org/10.1007/s11214-013-0029-z.

Han, Q., Fan, K., Cui, J., Wei, Y., Fraenz, M., Dubinin, E., et al. (2019). The relationship between photoelectron boundary and steep electron density gradient on Mars: MAVEN observations, *Journal of Geophysical Research: Space Physics*, *124*, 8015–8022. https://doi.org/10.1029/2019JA026739

Han, X., Fraenz, M., Dubinin, E., Wei, Y. J., Andrews, D. J., Wan, W., et al. (2014). Discrepancy between ionopause and photoelectron boundary determined from Mars Express measurements. *Geophysical Research Letters*, *41*, 8221–8227.

Jakosky, B., Lin, R. P., Grebowsky, J. M., Luhmann, J. G., Mitchell, D. F., Beutelschies, G., et al. (2015). The Mars Atmosphere and Volatile Evolution (MAVEN) mission. *Space Science Reviews*, *195*(1-4), 3–48. https://doi.org/10.1007/s11214-015-0139-x

Knudsen, W. C., Spenner, K., Whitten, R. C., Spreiter, J. R., Miller, K. L., & Noval, V. (1979). Thermal structure and major ion composition of the Venus ionosphere: First RPA results from Venus orbiter. *Science*, *203*, 757–763. https://doi.org/10.1126/science.203.4382.757

Lundin, R., Barabash, S., Andersson, H., Holmström, M., Grigoriev, A., Yamauchi, M., et al. (2004). Solar wind-induced atmospheric erosion at Mars: First results from ASPERA-3 on Mars Express. *Science*, *305*, 1933–1936. https://doi.org/10.1126/science.1101860

Lundin, R., Barabash, S., Holmstrom, M., Nilsson, H., Futaana, Y., Ramstad, R., et al. (2013). Solar cycle effects on the ion escape from Mars. *Geophysical Research Letters*, *40*, 6028–6032. https://doi.org/10.1002/2013GL058154

Mantas, G. P., & Hanson, W. B. (1979). Photoelectron fluxes in the Martian ionosphere. *Journal of Geophysical Research*, *84*, 369–385. https://doi.org/10.1029/JA084iA02p00369

Matsunaga, K., Seki, K., Brain, D. A., Hara, T., Masunaga, K., Mcfadden, J. P., et al. (2017). Statistical study of relations between the induced magnetosphere, ion composition, and pressure balance boundaries around Mars based on MAVEN observations. *Journal of Geophysical Research: Space Physics*, *122*, 9723–9737. https://doi.org/10.1002/2017JA024217

Mitchell, D. L., Lin, R. P., Mazelle, C., Rème, H., Cloutier, P. A., Connerney, J. E. P., et al. (2001). Probing Mars' crustal magnetic field and ionosphere with the MGS electron reflectometer. *Journal of Geophysical Research*, *106*, 23,419–23,428. https://doi.org/10.1029/2000JE001435

Mitchell, D. L., Lin, R. P., Reme, H., Crider, D. H., Cloutier, P. A., Connerney, J. E. P., et al. (2000). Oxygen auger electrons observed in Mars' ionosphere. *Geophysical Research Letters*, *27*, 1871–1874. https://doi.org/10.1029/1999GL010754

Morgan, D. D., Gurnett, D. A., Kirchner, D. L., Fox, J. L., Nielson, E., Plaut, J. J., & Picardi, G. (2008). Variations of Mars's ionospheric electron density from Mars Express radar soundings. *Journal of Geophysical Research*, *113*, A09303. https://doi.org/10.1029/2008JA013313

Morschhauser, A., Lesur, V., & Grott, M. (2014). A spherical harmonic model of the lithospheric magnetic field of Mars. *Journal of Geophysical Research: Planets*, *119*, 1162–1188. https://doi.org/10.1002/2013JE004555

21699402, 2020, 5, Downloaded from https://agupubs.onlinelibrary.wiley.com/doi/10.1029/2019JA027409 by University Of Iowa, Wiley Online Library on [17/11/2022]. See the Terms and Conditions (https://onlinelibrary.wiley.com/terms-and-conditions) on Wiley Online Library for rules of use; OA articles are governed by the applicable Creative Commons License

Nagy, A. F., Winterhalter, D., Sauer, K., Cravens, T. E., Brecht, S., Mazelle, C., et al. (2004). The plasma environment of Mars. *Space Science Reviews*, *111*, 33–114.

Picardi, G., Biccari, D., Seu, R., Plaut, J., Johnson, W. T. K., Jordan, R. L., et al. (2004). *MARSIS: Advanced radar for subsurface and ionosphere sounding, Mars Express: A European Mission to the Red Planet* (Vol. 1240, pp. 51–69). Noordwijk, Netherlands: ESA Publ. Division.

Rahmati, A., D. E. Larson, T. E. Cravens, R. J. Lillis, J. S. Halekas, J. P. McFadden, et al. (2018). Seasonal variability of neutral escape from Mars as derived from MAVEN pickup ion observations. Journal of Geophysical Research: Planets, 123, 1192-1202 https://doi.org/10.1029/2018JE005560.

Sanchez-Cano, B., Lester, M., Witasse, O., Milan, S. E., Hall, B. E. S., Cartacci, M., et al. (2016). Solar cycle variations in the ionosphere of Mars as seen by multiple Mars Express data sets. *Journal of Geophysical Research: Space Physics*, *121*, 2547–2568. https://doi.org/10.1002/2015JA022281

Schunk, R. W., & Nagy, A. F. (2009). *Ionospheres: Physics, plasma physics, and chemistry*. Cambridge: Cambridge University Press, Second Edition.

Trotignon, J. G., Bertucci, C., & Acuña, M. H. (2006). Martian shock and magnetic pile-up boundary positions and shapes determined from the Phobos 2 and Mars Global Surveyor data sets. *Planetary and Space Science*, *54*, 357–369.

Valeille, A., Combi, M. R., Bougher, S. W., Tenishev, V., & Nagy, A. F. (2009). Three- dimensional study of Mars upper thermosphere/ionosphere and hot oxygen corona: Solar cycle, seasonal variations, and evolution over history. *Journal of Geophysical Research*, *114*, E11006. https://doi.org/10.1029/2009JE003389

Vignes, D., Mazelle, C., Reme, H., Acuña, M. H., Connerney, J. E. P., Lin, R. P., et al. (2000). The solar wind interaction with Mars: Locations and shapes of the bow shock and magnetic pile-up boundary from the observations of the MAG/ER experiment onboard Mars Global Surveyor. *Geophysical Research Letters*, *27*, 49–52.

Vogt, M. F., Withers, P., Mahaffy, P. R., Benna, M., Elrod, M. K., Halekas, J. S., et al., and Jakosky, B. M, (2015), Ionopause-like density gradients in the Martian ionosphere: A first look with MAVEN. *Geophysical Research Letters*, 42, 8885-8893. https://doi.org/10.1002/2015GL065269.

Withers, P., Morgan, D. D., & Gurnett, D. A. (2014). Variations in peak electron densities in the ionosphere of Mars over a full solar cycle. *Icarus*. 251(1), 5-11. https://doi.org/10.1016/j.icarus.2014.08.008

Yamauchi, M., Hara, T., Lundin, R., Dubinin, E., Fedorov, A., Sauvaud, J. -A., et al. (2015). Seasonal variations of Martian pick-up ions: Evidence of breathing exosphere. *Planetary and Space Science*, *119*, 54–61. https://doi.org/10.1016/j.pss.2015.09.013

Zhang, M. H. G. and J. G. Luhmann (1992), Comparisons of peak ionosphere pressures at Mars and Venus with incident solar wind dynamic pressure. *Journal of Geophysical Research*, *97*, 1017–1025.

21699402, 2020, 5, Downloaded from https://agupubs.onlinelibrary.wiley.com/doi/10.1029/2019JA027409 by University Of Iowa, Wiley Online Library on [17/11/2022]. See the Terms and Conditions (https://onlinelibrary.wiley.com/terms-and-conditions) on Wiley Online Library for rules of use; OA articles are governed by the applicable Creative Commons License